Exact Medial Axis Computation for Circular Arc Boundaries

Oswin Aichholzer[1], Wolfgang Aigner[1], Thomas Hackl[1], and Nicola Wolpert[2]

[1] Institute for Software Technology, Graz University of Technology, Austria
[2] Faculty Geomatics, Computer Science and Mathematics,
Stuttgart University of Applied Sciences, Germany

Abstract. We propose a method to compute the algebraically correct medial axis for simply connected planar domains which are given by boundary representations composed of rational circular arcs. The algorithmic approach is based on the Divide-&-Conquer paradigm, as used in [2]. However, we show how to avoid inaccuracies in the medial axis computations arising from a non-algebraic biarc construction of the boundary. To this end we introduce the Exact Circular Arc Boundary representation (ECAB), which allows algebraically exact calculation of bisector curves. Fractions of these bisector curves are then used to construct the exact medial axis. We finally show that all necessary computations can be performed over the field of rational numbers with a small number of adjoint square-roots.

Keywords: medial axis, circular boundary, exact computation

1 Introduction

The *medial axis* is an important concept for shape description introduced by Blum [4]. We call a domain S in the plane a simple shape, if it is bounded by a non-selfintersecting closed curve ∂S. The medial axis of S is composed of the union of all center points of *maximal disks* inscribed in S. If S is simple then its axis has a tree-like structure. The following two definitions stem from [4]:

Definition 1. *Given a shape S, a disk $D \subseteq S$ is called maximal, if there does not exist a disk $D' \subseteq S$, $D' \neq D$, which contains D. We denote the set of all maximal disks with $MAT(S)$ (medial axis transform of S).*

Definition 2. *Given a shape S, its medial axis $MA(S)$ is defined as the union of all centers of maximal disks in S:*

$$MA(S) := \{c_D \mid D \in MAT(S), \text{ and } c_D \text{ is the center of } D\} \ .$$

The medial axis construction for shapes with simple boundary representations as straight lines or circular arcs is a field that has been tackled with various techniques. The Divide-&-Conquer approach used in [2] is a simple method for efficient axis computation, however, with some minor drawbacks. The biarc construction as described in [2] provides theoretical smoothness, that is however not representable by usual float or rational number types. Furtheron, degenerate branching points of the medial axis cannot be detected exactly. In particular, the correct representation of the medial axis curve is a challenging task if the boundary input data does not comply with certain (numerical or algebraic) quality criteria as being rational representable or providing algebraically smooth joints between arcs.

An important part of most medial axis algorithms is the bisector computation. This problem has been approached for various types of rational curves, but mostly relying on machine arithmetic as in [11, 7].

Our goal is to compute the algebraically correct medial axis. Thus, we have to cope with exact bisector computation of (arc-supporting) circles. For this purpose we require all arcs on the boundary, that are involved in the bisector computation, to be *rational*. Arcs which do not directly contribute to the medial axis, but describe a local curvature maximum and thus merely a leaf-point of the axis, are allowed to be rational square-root expressions (*rasqex*).

Integers are rasqex. If x and y are rasqex, so are $x + y$, $x - y$, $x \cdot y$, x/y and $\sqrt{x}$. Rasqex have exact comparison operators $=$, $<$, and $>$, realized in LEDA [6, 14] or the Core library [13, 16]. Actually, these two packages are able to represent arbitrary k-th root numbers, what is more than we need. For our purposes the *FieldWithSqrt* concept as provided by the CGAL library [1] is sufficient.

Several details of our algorithm, e.g. bisectors and tritangent circles, are similar to those needed for the construction of an Apollonius diagram, as examined extensively in the work of Emiris and Karavelas [8]. They show that the operations allowed in the rasqex number type are sufficient to compute all predicates. Similar efforts have been made for ellipses and even more general smooth convex sites [9, 10]. Beside the similarities there are serveral additional aspects we have to take into account for our approach. First, the medial axis construction needs parts from the underlying bisectors different from the ones needed for the Apollonius diagram. Second, while in [8] an incremental approach is pursued, we intend to show that all steps of our Divide-&-Conquer algorithm can be accomplished with rasqex numbers as well, a fact that is not obvious. Furthermore, as opposed to the Apollonius diagram, we do not deal with single sites and complete circles, but one closed curve composed of circular arcs representing a planar shape. In this context we consider boundaries that are at least C^1-smooth to define an *Exact Circular Arc Boundary* or *ECAB*. (The extension to non-smooth boundaries only requires an extension of the cases that may occur for bisector computation.) See Section 2 for detailed definitions.

Given an *ECAB*, the divide-part of the algorithm presented in [2] is applied (overview in Section 3) with some minor modification of the construction of the *dividing disks* (Section 4), as they are crucial for the final reassembling of the medial axis. The main bisector calculus takes place when arriving at the base cases which terminate the decomposition process. Pairs of (rational) arcs are adequately chosen, and the bisectors of their supporting circles are computed.

It is shown in Section 5 that the bisectors are algebraic curves of degree 4 over the rational numbers $\mathbb{Q}$, which can be expressed as the product of two quadratic polynomials (conics) over a simple extension field of $\mathbb{Q}$. The center points of the arcs stemming from the dividing disks (called *artificial arcs*) lie on the bisectors, and are used to isolate those parts of the conic curves which contribute to the partial medial axes of specific base cases. Details about these base cases are discussed in Section 6, representing the conquer-part of the algorithm.

2 Exact Circular Arc Boundary

We define a circular boundary representation which fits our needs for an exact bisector and medial axis construction. This requires some definitions, starting with *rational circles*. Let $\mathbb{Q}$ denote the set of rational numbers.

Definition 3. *For a circle C with center c the following definitions are equivalent:*

$$C \text{ is a rational circle} \iff c \in \mathbb{Q}^2 \quad \text{and} \quad \exists u \in C : u \in \mathbb{Q}^2 \tag{1}$$

$$\iff \exists u, v, w \in \mathbb{Q}^2 : u, v, w \in C \; . \tag{2}$$

Note that the squared radius of a rational circle is rational. It is also well-known that on a rational circle C points with rational coordinates are lying dense (see [15]). This means that near an arbitrary point p on C and for any $\epsilon > 0$ one can find a rational point in an ϵ-environment around p, that lies on C. We say that an arc is *rational*, if its supporting circle and its two endpoints are rational. By extending to rasqex numbers, we can now define *rasqex circles* as a superset of rational circles.

Definition 4. *For a circle C with center c and squared radius r the following definitions are equivalent:*

$$C \text{ is a rasqex circle} \iff c \text{ and } r \text{ are rasqex} \; .$$

An arc is *rasqex*, if its supporting circle and its two endpoints are rasqex. A rational circle is always a rasqex one, but not vice versa. For our C^1-boundary representation we want to rely on rational circles as much as possible, but to build a C^1-smooth boundary consisting exclusively of rational arcs means a severe restriction. We therefore soften our demands by allowing rasqex arcs whenever they are not directly contributing to bisector calculation. This is true for arcs which describe a *local curvature maximum*, as such a maximum always defines a leaf-point of the medial axis which just represents the endpoint of a medial axis curve. This means such an arc does not contribute to any bisector computation later on (Section 5), only its center point is eventually required for point location (Section 6). According boundary construction rules are given in Section 7.

Definition 5. *Consider a C^1-circular arc boundary representation. An arc that constitutes a local curvature maximum, and thus a leaf point of the medial axis, has to be at least rasqex. If all other arcs are rational, then we call this structure an Exact Circular Arc Boundary (ECAB).*

Note that the restriction to C^1 is not a necessary one. For general circular arc boundaries however we have to deal with more base cases and with bisector construction between points and circles. This does not pose any problems concerning computation, but is left aside for reasons of lucidity.

3 The Divide-&-Conquer Algorithm

We are interested in computing the medial axis for a given ECAB boundary. As our approach is closely related to the work introduced in [2] we first give an overview here. The algorithm is based on the Divide-&-Conquer paradigm. The dividing step consists of finding a random disk $D \in MAT(S)$ (called *dividing disk*) and decomposing S, with the help of D, into sub-shapes. The latter is done by splitting the boundary, adding *artificial arcs* that originate from D, and rearranging the *original arcs*. After this has been applied recursively, down to predefined base cases, the merge step is a simple concatenation of the partial axes at the center points of the dividing disks, as they are guaranteed to lie on the original medial axis. For a list of base cases that may occur for C^1-smooth boundaries, see Figure 3. We leave the basic algorithmic approach almost unchanged. But with the help of the properties of the ECAB structure (as opposed to numerical biarc constructions), and by modifying a few specific steps, a mathematically correct representation of the medial axis is made possible:

- The construction of a dividing disk has to be done with care, to take advantage of the properties of rational arcs. The centers of the dividing disks play a more important role, as they are required to lie exactly on the bisector curves for segment confinement. This is discussed in Section 4.
- The bisector computation is now done in an algebraic way, avoiding any numerical errors. The whole computation can be done over the field of rational numbers with only a few adjoint square-roots, as shown in Section 5.
- The handling of the base cases is more sophisticated, however the algebraic approach allows us to detect degenerate constellations more easily (Section 6).

4 Constructing Dividing Disks

Dividing disks, being maximal disks as defined in Section 1, are required for the recursive decomposition of a shape S. A general maximal disk has two contact points on ∂S, which lie on two different arcs when dealing with an ECAB.

As in [2] we start by choosing a random arc p on the boundary. The only limitation is that p must not define a local curvature maximum, meaning it does not induce a leaf-point of the medial axis. The ECAB structure then tells us that p is rational and thus we can choose a rational point t_p as close to an arbitrary point on p as we see fit. See [5] for a detailed algorithm and implementation on how to choose such a point. For every arc $q \neq p$ of ∂S we construct the disk that

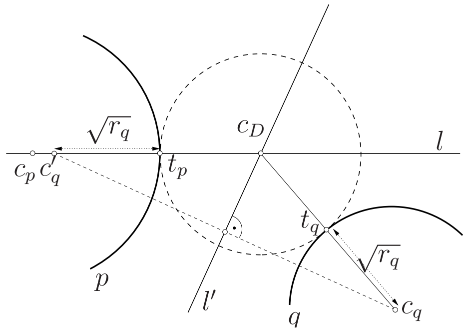

Fig. 1. Construction of a disk that is tangent to two arcs.

touches p at t_p and is tangent to q (see Figure 1). First we construct the line l passing through the center c_p of the supporting circle of p and t_p. The center c_D of the maximal disk we are looking for has to be on l. As can be decided by the signs of curvature of p and q, one of the two points on l being at distance $\sqrt{r_q}$ (radius of the supporting circle of q) from t_p is denoted with c'_q. This point c'_q forms, together with c_D and c_q, an isosceles triangle. The bisector l' between c_q and c'_q also contains c_D, which means that c_D is the intersection point of l and l'. From all $q \neq p$ only one induces a disk (the smallest one) that lies completely inside S. This is the sought-after dividing disk D. The use of the ECAB structure guarantees certain algebraic properties of D. As the point c_p as well as t_p are rational, also the line l is rational. The value $\sqrt{r_q}$ is not rational in general, as a consequence so isn't c'_q. However, $c'_q \in \mathbb{Q}(\sqrt{r_q})^2$. Therefore also the point of intersection between l and l', being the center of D, is in this extension field. Values in $\mathbb{Q}(\sqrt{r_q})$ can be represented exactly by the rasqex numbers, which makes later point location on the bisector curves convenient (see Section 5.2 and 6).

Furthermore, we note that the (rasqex) artificial arcs, stemming from the (rasqex) boundary circle of a dividing disks, always describe a local curvature maximum when used to extend the partial shapes. This is coherent with the definition of the ECAB-structure in Section 2.

5 Bisector Computation and Point Location

5.1 Bisector Computation

We next show how to compute the bisector between two rational arcs. Let C_p and C_q be the supporting circles of the two arcs with centers c_p and c_q and squared radii r_p and r_q, respectively:

$$C_p(x, y) := (x - (c_p)_x)^2 + (y - (c_p)_y)^2 - r_p$$
$$C_q(x, y) := (x - (c_q)_x)^2 + (y - (c_q)_y)^2 - r_q \ .$$

As before, we assume $c_p, c_q \in \mathbb{Q}^2$ and $r_p, r_q \in \mathbb{Q}$.

Definition 6. *The* bisector curve *between the two circles* C_p *and* C_q *consists of all points* (x, y) *in the plane for which*

$$\big||(x,y)-c_p| \pm \sqrt{r_p}\big| = \big||(x,y)-c_q| \pm \sqrt{r_q}\big|$$

Roughly said, this bisector curve consists of all center points of circles, which share exactly one point (of tangency) with C_p and C_q respectively.

Theorem 1. *The bisector curve of the two circles* C_p *and* C_q *factors into two curves* $B_1(x, y) = 0$ *and* $B_2(x, y) = 0$ *with*

$$B_1(x,y) = (d_1^2 + d_2^2 - r^2)^2 - 4d_1^2 d_2^2 \ \in \ \mathbb{Q}(\sqrt{r_p r_q})[x,y] \tag{3}$$
$$B_2(x,y) = (d_1^2 + d_2^2 - \tilde{r}^2)^2 - 4d_1^2 d_2^2 \ \in \ \mathbb{Q}(\sqrt{r_p r_q})[x,y] \tag{4}$$

with $d_1 := d_1(x, y) := |(x, y)-c_p|$, $d_2 := d_2(x, y) := |(x, y)-c_q|$, $r := \sqrt{r_p}-\sqrt{r_q}$, *and* $\tilde{r} := \sqrt{r_p} + \sqrt{r_q}$.

Proof. For the bisector-curve there are two cases:

Case 1
$$\begin{cases} \begin{cases} d_1 + \sqrt{r_p} = d_2 + \sqrt{r_q} \ \vee d_1 - \sqrt{r_p} = d_2 - \sqrt{r_q} \\ \vee \ d_1 + \sqrt{r_p} = -d_2 + \sqrt{r_q} \vee d_1 - \sqrt{r_p} = -d_2 - \sqrt{r_q} \end{cases} \\ \Longleftrightarrow \begin{cases} d_1 - d_2 = -r \vee d_1 - d_2 = r \\ \vee \ d_1 + d_2 = -r \vee d_1 + d_2 = r \end{cases} \qquad |\_^2 \\ \Longleftrightarrow d_1^2 + d_2^2 - r^2 \ = \ 2d_1 d_2 \ \ \vee \ \ d_1^2 + d_2^2 - r^2 \ = \ -2d_1 d_2 \qquad |\_^2 \\ \Longleftrightarrow (d_1^2 + d_2^2 - r^2)^2 \ = \ 4d_1^2 d_2^2 \end{cases}$$

This is exactly the equation for $B_1(x, y) = 0$. Similar for $B_2(x, y) = 0$:

Case 2
$$\begin{cases} \begin{cases} d_1 + \sqrt{r_p} = -d_2 - \sqrt{r_q} \vee d_1 - \sqrt{r_p} = -d_2 + \sqrt{r_q} \\ \vee \ d_1 + \sqrt{r_p} = d_2 - \sqrt{r_q} \ \ \vee d_1 - \sqrt{r_p} = d_2 + \sqrt{r_q} \end{cases} \\ \Longleftrightarrow (d_1^2 + d_2^2 - \tilde{r}^2)^2 \ = \ 4d_1^2 d_2^2 \end{cases}$$

Since $d_1^2, d_2^2 \in \mathbb{Q}[x, y]$, $\tilde{r}^2 = (\sqrt{r_p} + \sqrt{r_q})^2 = r_p + 2\sqrt{r_p r_q} + r_q \in \mathbb{Q}(\sqrt{r_p r_q})$, and $r^2 = (\sqrt{r_p} - \sqrt{r_q})^2 = r_p - 2\sqrt{r_p r_q} + r_q \in \mathbb{Q}(\sqrt{r_p r_q})$, it follows that $B_1(x, y), B_2(x, y) \in \mathbb{Q}(\sqrt{r_p r_q})[x, y]$. □

From now on B_1 and B_2 denote the curves described by $B_1(x, y) = 0$ and $B_2(x, y) = 0$ respectively.

Theorem 2. B_1 *and* B_2 *in Theorem 1 are conics, i.e., planar curves of degree two.*

Proof. We will prove that B_1 and B_2 are conics when the centers of the circles C_p and C_q lie on the x-axis and symmetrically on both sides of the y-axis:

$$C_p(x,y) := (x+d)^2 + y^2 - r_p, \quad C_q(x,y) := (x-d)^2 + y^2 - r_q \ .$$

This is no restriction because every pair of circles with d being half the distance between their two center points can be moved to this position by rotation and translation. B_1 and B_2 are then subject to the same transformation which does not change their degrees.

For C_p and C_q being in this special position it is

$$\begin{aligned} d_1^2 = d_1^2(x,y) &= \mid (x,y) - c_p \mid^2 = \mid (x,y) - (-d,0) \mid^2 = (x+d)^2 + y^2 \\ d_2^2 = d_2^2(x,y) &= \mid (x,y) - c_q \mid^2 = \mid (x,y) - (d,0) \mid^2 = (x-d)^2 + y^2 \ . \end{aligned}$$

This yields for the two cases

$$\textit{Case 1} \quad \begin{cases} (d_1^2 + d_2^2 - r^2)^2 = 4d_1^2 d_2^2 \\ \Longleftrightarrow (x^2 + d^2 + y^2 - \frac{r^2}{2})^2 = ((x+d)^2 + y^2)((x-d)^2 + y^2) \\ \Longleftrightarrow 0 = 4x^2d^2 - x^2r^2 - d^2r^2 - y^2r^2 + \frac{r^4}{4} \end{cases}$$

This is the quadratic equation for B_1.

$$\textit{Case 2} \quad \begin{cases} (d_1^2 + d_2^2 - \tilde{r}^2)^2 = 4d_1^2 d_2^2 \\ \Longleftrightarrow 0 = 4x^2d^2 - x^2\tilde{r}^2 - d^2\tilde{r}^2 - y^2\tilde{r}^2 + \frac{\tilde{r}^4}{4} \end{cases}$$

This is the quadratic equation for B_2. □

Altogether this means that the bisector of the two circles C_p and C_q in our original coordinate system factors into two conics over the field $Q_{pq} = \mathbb{Q}(\sqrt{r_p r_q})$, which is in rasqex.

Corollary 1. *Each of B_1 and B_2 is either a hyperbola or an ellipse or a pair of identical lines.*

Proof. Looking further at the equations for B_1 and B_2 in the special case where the center-points lie on the x-axis we first observe that B_1 and B_2 are the two conics described by

$$B_1(x,y) := bx^2 - ay^2 - ab, \qquad B_2(x,y) := \tilde{b}x^2 - \tilde{a}y^2 - \tilde{a}\tilde{b}$$

with

$$a = \frac{(\sqrt{r_p} - \sqrt{r_q})^2}{4} = \frac{r^2}{4}, \qquad b = d^2 - a = d^2 - \frac{r^2}{4}$$

and

$$\tilde{a} = \frac{(\sqrt{r_p} + \sqrt{r_q})^2}{4} = \frac{\tilde{r}^2}{4}, \qquad \tilde{b} = d^2 - \tilde{a} = d^2 - \frac{\tilde{r}^2}{4} \ .$$

First consider B_1. If $r_p = r_q$ we have $a = 0$, $b = d^2$ and $B_1(x,y) = d^2x^2$ consists of two identical lines along the y-axis. If $r_p \neq r_q$ it is true that $a > 0$ and

$$b > 0 \ \Leftrightarrow \ d^2 > \frac{r^2}{4} \ \Leftrightarrow \ 4d^2 > (\sqrt{r_p} - \sqrt{r_q})^2 \ \Leftrightarrow \ 2d > |\sqrt{r_p} - \sqrt{r_q}| \ .$$

That means,

– if $2d > |\sqrt{r_p} - \sqrt{r_q}|$, then $b > 0$ and B_1 is an hyperbola,
– if $2d = |\sqrt{r_p} - \sqrt{r_q}|$, then $b = 0$ and $B_1(x, y) = -ay^2$ consists of two identical lines along the x-axis,
– if $2d < |\sqrt{r_p} - \sqrt{r_q}|$, then $b < 0$ and B_1 is an ellipse.

For B_2 we always have $\tilde{a} > 0$ and

$$\tilde{b} > 0 \;\Leftrightarrow\; d^2 > \frac{\tilde{r}^2}{4} \;\Leftrightarrow\; 4d^2 > (\sqrt{r_p} + \sqrt{r_q})^2 \;\Leftrightarrow\; 2d > \sqrt{r_p} + \sqrt{r_q}\ .$$

– The two circles C_p and C_q do not intersect iff $2d > \sqrt{r_p} + \sqrt{r_q}$. In this case $\tilde{b} > 0$ and B_2 is a hyperbola.
– C_p and C_q touch tangentially iff $2d = \sqrt{r_p} + \sqrt{r_q}$. Then $B_2(x, y) = -\tilde{a}y^2$ consists of two identical lines along the x-axis.
– C_p and C_q intersect iff $2d < \sqrt{r_p} + \sqrt{r_q}$. In this case $\tilde{b} < 0$ and B_2 is an ellipse. □

5.2 Medial Axis Representation and Point Location

In order to compute and represent the medial axis of the exact circular arc boundary we must be able to analyze a bisector-conic over the extension field Q_{pq}. This means that in a so called *one-curve analysis* we will divide a bisector-conic B, described by $B(x, y) \in \mathbb{Q}(\sqrt{r_p r_q})[x, y] = Q_{pq}[x, y]$, into x-monotone arcs. This is not difficult and works analogously to the one-curve analysis of a conic over $\mathbb{Q}$ described in [3]. The bisector-conic B is split at its x-extreme points, that are points where $B(x, y)$ and the partial derivative $B(x, y)_y = \frac{\partial B(x,y)}{\partial y}$ vanish simultaneously. If the bisector-conic consists of a pair of identical lines, we make the defining polynomial square-free. Now every resulting x-monotone arc can be represented by a tuple $([le, ri], nr)$, where le and ri are the x-coordinates of the left and right endpoint, respectively. Since le and ri are roots of quadratic polynomials over $Q_{pq}[x]$, they can be represented by rasqex numbers. The branch number nr is either 0 or 1 and indicates which of the two x-monotone arcs of the curve above the x-interval $[le, ri]$ is meant.

As described in Section 4, one major step is point-location. For a given point $u = (u_x, u_y)$, the coordinates of which are rasqex, we have to determine the x-monotone arc of B_1 or B_2 it lies on. First of all we check whether u lies on B_1 or B_2 by testing

$$B_1(u_x, u_y) = 0 \quad \text{or} \quad B_2(u_x, u_y) = 0\ . \tag{5}$$

Since all the numbers in $B_1(u_x, u_y)$ and $B_2(u_x, u_y)$ are rasqex numbers, the exact test for zero can be realized by using the equality operator of the rasqex numbers. Let us assume that p lies on B_1. Next we use the $<$-operator of the rasqex numbers to determine the two x-monotone arcs of B_1 for which

$$le \leq u_x \leq ri\ . \tag{6}$$

The last step is to determine whether u lies on the upper or lower branch, i.e., algebraically whether u_y is the greater or smaller root of the polynomial

$B_1(u_x, y)$. Since $B_1(u_x, y)$ is a quadratic polynomial the coefficients of which are rasqex, its two roots r_1 and r_2 can be computed symbolically by introducing a new square-root. Now we have to check whether

$$u_y - r_1 = 0 \quad \text{or} \quad u_y - r_2 = 0 \; . \tag{7}$$

Again this can be done by using rasqex numbers. Notice that in cases where locally around u neither the second bisector-conic nor the second arc pass by and all x-extreme points are far away, the three steps for point-location can be sped up by using isolating intervals for u_x and u_y and evaluating the expressions in (5), (6) and (7) with interval arithmetic, if desired.

5.3 Confining the Partial Axis

In our construction, the medial axis is computed as the union of bisector-conic segments. Each conic segment is limited by center points of artificial arcs. Consider the case where the bisector of two rational arcs on the circles C_p and C_q contribute to the medial axis, see for example Figure 3 case (b). The coordinates of the limiting center points of the artificial arcs are rasqex. With the algorithm described above the center points can be located on x-monotone arcs of the bisector-conic. If the bisector-conic is a line or hyperbola, the two center-points uniquely define the part of the medial axis we are interested in, possibly as a concatenation of x-monotone arcs. If the underlying bisector-conic is an ellipse, we have two possibilities for the partial axis. In this case we choose an additional rational point on one rational arc, say on C_p. With the algorithm from Section 4 we construct a third point on the bisector-conic. For the partial axis we choose the part of the bisector-curve between the two center points which contains this new point.

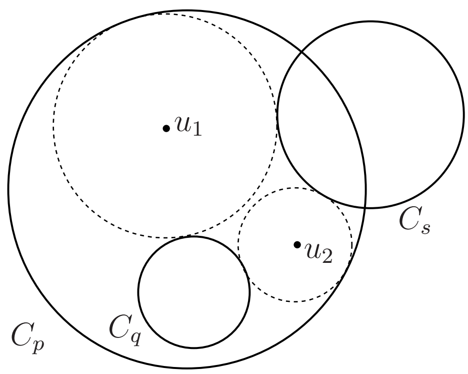

Fig. 2. Two tritangent circles resulting from one line of similitude of the Gergonne construction. $(\varphi(u_1, C_p), \varphi(u_1, C_q), \varphi(u_1, C_s)) = (\varphi(u_2, C_p), \varphi(u_2, C_q), \varphi(u_2, C_s)) = (1, 0, 0)$.

5.4 Center Points of Tritangent Circles

The center points of (at least) tritangent circles, being the branching points of the medial axis, are another kind of points which are needed for the confinement of the axis. We will show that the coordinates of such points are rasqex too, if the three defining circles are rational. A bisector curve between two rational circles is an algebraic curve of degree 4, and the branching point is one of the intersection points where all three bisectors between three circles meet.

There exist two different possibilities how a point on a bisector-curve may describe tangency at its footpoint on a defining circle.

Definition 7. *Consider a bisector-curve B and one of its two defining circles C. For a point $t \in B$ let t'_C be its unequivocal footpoint on C and Γ_C the open region bounded by C. Then we define the function $\varphi(t, C)$ on B as follows:*

$$\varphi(t, C) = \begin{cases} 0 & \textit{if} \quad \overline{t\, t'_C} \cap \Gamma_C = \emptyset \\ 1 & \textit{otherwise} \end{cases}$$

Roughly speaking $\varphi(t, C)$ is 0 if the circle with center t and radius $\overline{t\, t'_C}$ is "outer"-tangent to C, and 1 otherwise (see also Figure 2). As proved in Section 5 every bisector B consists of two conic curves, B_1 and B_2. By construction, the points of these two conics have certain properties concerning $\varphi(.,.)$ which we investigate next.

Lemma 1. *Consider the bisector B consisting of the two bisector-conics B_1 and B_2 and its two defining circles C_p and C_q, then*

$$\forall t \in B_1 \ : \ (\varphi(t, C_p), \varphi(t, C_q)) \in \{(0,0), (1,1)\} \tag{8}$$

$$\forall t \in B_2 \ : \ (\varphi(t, C_p), \varphi(t, C_q)) \in \{(0,1), (1,0)\} \ . \tag{9}$$

Proof. As derived in the proof of Theorem 1, for every point t on B_1 it holds that

$$\begin{aligned} & |t - c_p| + \sqrt{r_p} = |t - c_q| + \sqrt{r_q} \lor |t - c_p| - \sqrt{r_p} = |t - c_q| - \sqrt{r_q} \\ \lor \ \ & |t - c_p| + \sqrt{r_p} = -|t - c_q| + \sqrt{r_q} \lor |t - c_p| - \sqrt{r_p} = -|t - c_q| - \sqrt{r_q} \ . \end{aligned}$$

This leads to

$$\begin{aligned} & \varphi(t, C_p) = 1 \land \varphi(t, C_q) = 1 \lor \varphi(t, C_p) = 0 \land \varphi(t, C_q) = 0 \\ \lor \ \ & \varphi(t, C_p) = 1 \land \varphi(t, C_q) = 1 \lor \varphi(t, C_p) = 1 \land \varphi(t, C_q) = 1 \ . \end{aligned}$$

For every point x on B_2 it is

$$\begin{aligned} & |t - c_p| + \sqrt{r_p} = -|t - c_q| - \sqrt{r_q} \lor |t - c_p| - \sqrt{r_p} = -|t - c_q| + \sqrt{r_q} \\ \lor \ \ & |t - c_p| + \sqrt{r_p} = |t - c_q| - \sqrt{r_q} \lor |t - c_p| - \sqrt{r_p} = |t - c_q| + \sqrt{r_q} \ . \end{aligned}$$

This leads to

$$\begin{aligned} & \text{undefined} \lor \varphi(t, C_p) = 0/1 \land \varphi(t, C_q) = 1/0 \\ \lor \ \ & \varphi(t, C_p) = 1 \land \varphi(t, C_q) = 0 \lor \varphi(t, C_p) = 0 \land \varphi(t, C_q) = 1 \ . \end{aligned}$$

□

We are interested in the situation where three rational circles C_p, C_q and C_s are given. They define three bisectors: $B^{'}$ between C_p and C_q, $B^{''}$ between C_q and C_s and $B^{'''}$ between C_p and C_s. A branching point u, being the center of a tritangent circle, lies on all three bisectors and so $\varphi(u,.)$ is well defined for all three circles. Let

$$\Phi(u) := (\varphi(u, C_p), \varphi(u, C_q), \varphi(u, C_s)) \ . \tag{10}$$

Observation 1 *Depending on which bisector-conics intersect in a branching point u, we distinguish between four different sets of contact tuples. For all other possible combinations of three bisector-conics a common intersection point is impossible.*

$$u \in B_1^{'} \cap B_1^{''} \cap B_1^{'''} \quad \Rightarrow \quad \Phi(u) \in \{(0,0,0),(1,1,1)\} \tag{11}$$

$$u \in B_1^{'} \cap B_2^{''} \cap B_2^{'''} \quad \Rightarrow \quad \Phi(u) \in \{(0,0,1),(1,1,0)\} \tag{12}$$

$$u \in B_2^{'} \cap B_1^{''} \cap B_2^{'''} \quad \Rightarrow \quad \Phi(u) \in \{(1,0,0),(0,1,1)\} \tag{13}$$

$$u \in B_2^{'} \cap B_2^{''} \cap B_1^{'''} \quad \Rightarrow \quad \Phi(u) \in \{(1,0,1),(0,1,0)\} \tag{14}$$

For example, considering case (11), if $u \in B_1^{'} \cap B_1^{''} \cap B_1^{'''}$, then due to Lemma 1 it holds that

$$\begin{aligned} &(\varphi(u, C_p), \varphi(u, C_q)) \in \{(0,0),(1,1)\} \\ \wedge\ &(\varphi(u, C_q), \varphi(u, C_s)) \in \{(0,0),(1,1)\} \\ \wedge\ &(\varphi(u, C_p), \varphi(u, C_s)) \in \{(0,0),(1,1)\} \ . \end{aligned}$$

This is only true if $\varphi(u, C_p) = \varphi(u, C_q) = \varphi(u, C_s) = 0$ or $\varphi(u, C_p) = \varphi(u, C_q) = \varphi(u, C_s) = 1$. The other cases work analogously.

The construction of all possible circles that are tangent to three given circles is a much discussed topic, with various possible ways of solution (see e.g. [12]). It is folklore that there exist at most 8 different tritangent circles in this case. The Gergonne construction, named after french mathematician Joseph Diaz Gergonne, is based on inverse geometry and uses so called *lines of similitude*. For three circles in general position, there exist 4 lines of similitude. Each line induces at most 2 tritangent circles, which can both together be assigned to one specific case (11) to (14) from Observation 1. Note however, that e.g. for case (13) there may be two solutions of the form $(1,0,0)$ and none for $(0,1,1)$ (see Figure 2 for an example).

This means that constellations of three bisector-conics as shown in Observation 1 have at most two common intersection points. The x-coordinates of the intersection points of two of the three conics are roots of a degree four polynomial P_1 (which can be derived by a resultant computation). For another pair of conics we obtain another polynomial P_2. We now isolate the common x-components by computing the greatest common divisor $P' = \gcd(P_1, P_2)$. As at most two common solutions may exist, P' is a quadratic polynomial. Its roots can be represented exactly by rasqex numbers.[3] The same way the possibly two y-coordinates can be computed. This shows that the coordinates of the center points of tritangent circles can be represented as rasqex numbers and we get $2 \cdot 2 = 4$ candidates for them.

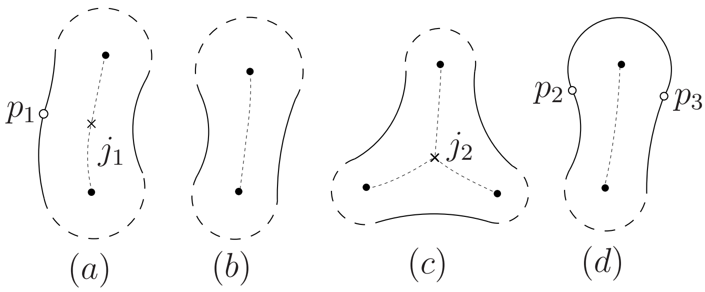

Fig. 3. The four combinatorial different base cases that may occur for the ECAB structure, as described in Section 6.

6 Partial Axis Construction

In general, four combinatorially different base cases with ≤ 3 original arcs may stem from the iterative dividing process (Figure 3). The medial axes of these base cases are then represented directly by portions of algebraically simple circle bisectors. After the mathematical elaboration in Section 5 we now have a closer look at the combinatorial composition of the axes.

(a) The medial axis of base case (a) in Figure 3 consists of parts of the two bisectors between one of the two arcs incident to p_1 and the opposite arc. As we have a smooth transition at the rational point p_1, the two resulting bisector segments have a tangent point at the joint point j_1, which has rasqex coordinates. Together with the (rasqex) center points of the artificial arcs, j_1 is used to confine the required parts of the conic bisectors as described in Section 5.3.
(b) The axis is the segment of the two original arcs' bisector, which is confined by the two center points of the artificial arcs, see Section 5.3.
(c) The base case of this form represents the generic case for branching points of the medial axis. Its axis is composed of bisector parts from all pair constellations of original arcs. Let C_p, C_q and C_s be the three circles the original

[3] In the special case where P_1 and P_2 have more than two common roots due to covertical intersection points, we shear the coordinate system, compute the center points of the tritangent circles in the sheared system and transform the result back to the original coordinate system.

arcs lie on. For isolation of these segments, in addition to the three artificial center points, the intersection point j_2 has to be identified. How to compute the potential coordinates of such a point, which are also rasqex, is shown in Section 5.4. Finally we choose the correct intersection point among the computed ones by computing additional points on the bisector curves and following them starting at the center point of an artificial arc.

(d) Bisector construction is done as in case (b). However, unlike in case (b), one of the two confining points is not an artificial center point, but a center point of an original arc which represents a leaf point of the medial axis structure.

An arbitrary variation of the case depicted in Figure 4 may arise as a degenerate exception, which is an occurrence of an axis branching, where more than three bisectors meet in one point. For our dividing process this means that we arrive at a shape, whose boundary is an alternating sequence of artificial and original arcs. Here no generic dividing disk exists that would lead to combinatorially smaller partial shapes.

Granted algebraic correctness, as is the case in our setting, such degenerate cases can be detected easily: whenever an alternating arc sequence is recognized we compute the bisectors of all pairs of arcs which are only separated by one artificial arc. If all these bisectors intersect in one single point then a degenerate case has occured. Computation is based on the principle introduced in Section 5.4, meaning that again rasqex numbers are sufficient for exact calculation. This guarantees a correct indication of such a case which then can be handled accordingly. This elegant and intuitive handling of degnerate cases is one of the main improvements over the numerical afflicted approach in [2].

For the axis construction the bisector curves between original arcs that are neighbored via a single artificial arc are of interest. They all intersect in one common point which is, together with the center points of the artificial arcs, required for the segment confinement.

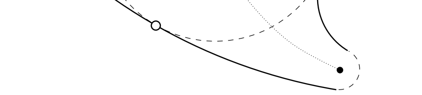

Fig. 4. Degenerate case example.

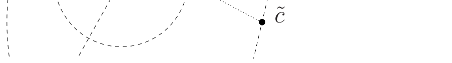

Fig. 5. Boundary construction which satisfies ECAB properties.

7 ECAB Construction

Our approach works on shapes S whose boundary ∂S is an ECAB. Thus in this final chapter we present a simple construction to obtain such a shape. In this construction only one single arc cannot be chosen rational but has to be rasqex. In accordance to the defintion of ECAB we shift this rasqex arc to a region where the curvature has a local maximum and therefore the medial axis has a leaf-point.

1. We start by choosing two rational points which represent the center of a circle and one endpoint of an arc on it (c_0 and p_0 in Figure 5). This circle is rational with respect to our definition in Section 2.
2. On the (rational) line through c_0 and p_0 we choose another rational point c_1, being the center of the next circle.
3. As c_1 and p_0 are rational, we can choose the next rational point p_1 in any ϵ-neighborhood around an arbitrary point on the circle with center c_1 and radius $\|c_1 - p_0\|$.
4. We repeat the last two steps until we arrive at the closing circle which has to represent a local curvature maximum of the boundary.
5. It is in general not possible to find a rational closing circle. But following the construction of a maximal disk as described in Section 4 we obtain a rasqex arc with the supporting circle centered at c' and with radius $\|c' - p'\|$.

Note: If the closing arc resulting from this ECAB construction, which is generally not rational, is treated like an artificial arc, then it can be handled without any further modification as part of the base cases depicted in Figure 3.

8 Conclusion

We showed that, given a boundary essentially composed of rational arcs (ECAB), the Divide-&-Conquer approach for medial axis construction from [2] can be adapted for algebraically exact calculation. Furthermore, encouraged by [8], we were able to show that the rasqex number type is sufficient for all arising computations. Intermediate steps and procedures are discussed in detail, and a construction guide for a simple ECAB is provided. What is missing so far is an analysis of the degrees of the geometric predicates involved in our computation. This is left as a topic for future research.

An extension to circular boundaries with non-differentiable arc joints only causes an increase of base and bisector cases (see also [2]). The same applies for straight line segments, which also introduce parabolic curves to the axis. Exact computation for boundary representations with curves of algebraically higher degree may be a topic for future work, although the bisector complexity grows considerably in this context.

We would like to point out again, that the self-contained representation by rasqex numbers is a beneficial one. Correctness of the result and exactness during computation (allowing e.g. the efficient detection and handling of degenerate cases) are achieved by applying only moderate changes to the original (floating point) algorithm. We think that with the exact computability of the medial axis the algorithm recommends itself for implementation in geometric libraries as CGAL [1].

References

1. CGAL, Computational Geometry Algorithms Library, http://www.cgal.org
2. Aichholzer, O., Aigner, W., Aurenhammer, F., Hackl, T., Jüttler, B., Rabl, M.: Medial Axis Computation for Planar Free-Form Shapes. Computer Aided Design 41(5), 339–349 (2009)
3. Berberich, E., Eigenwillig, A., Hemmer, M., Hert, S., Mehlhorn, K., Schömer, E.: A Computational Basis for Conic Arcs and Boolean Operations on Conic Polygons. In: ESA 2002. LNCS, vol. 2461, pp. 174–186. Springer, Heidelberg (2002)
4. Blum, H.: A Transformation for Extracting New Descriptors of Shape. In: Wathen-Dunn, W. (editor) Models for the Perception of Speech and Visual Form, pp. 362–380. MIT Press, Cambridge (1967)
5. Burnikel, C.: Rational Points on Circles. Research Report MPI-I-98-1-023. Max-Planck-Institut für Informatik, Saarbrücken (1998)
6. Burnikel, C., Funke, S., Mehlhorn, K., Schirra, S., Schmitt, S.: A Separation Bound for Real Algebraic Expressions. In: ESA 2001. LNCS, vol. 2161, pp. 154–265. Springer Heidelberg (2001)
7. Elber, G., Kim, M.-S.: Bisector Curves of Planar Rational Curves. Computer-Aided Design 30(14), 1089–1096 (1998)
8. Emiris, I.Z., Karavelas, M.I.: The Predicates of the Apollonius Diagram: Algorithmic Analysis and Implementation. Computational Geometry 33(1-2), 18–57 (2006)
9. Emiris, I.Z, Tsigaridas, E.P., Tzoumas, G.M.: Exact Delaunay Graph of Smooth Convex Pseudo-circles: General Predicates, and Implementation for Ellipses. In: SIAM/ACM Joint Conference on Geometric and Physical Modeling 2009, pp. 211–222. ACM, New York (2009)
10. Emiris, I.Z, Tzoumas, G.M.: Exact and Efficient Evaluation of the Incircle Predicate for Parametric Ellipses and Smooth Convex Objects. Computer-Aided Design 40(6), 691–700 (2008)
11. Hanniel, I., Muthuganapathy, R., Elber, G., Kim, M.-S.: Precise Voronoi Cell Extraction of Free-form Rational Planar Closed Curves. In: SPM 2005, pp. 51–59. ACM, New York (2005)
12. Kunkel, P.: The Tangency Problem of Apollonius: Three Looks. BSHM Bulletin: Journal of the British Society for the History of Mathematics 22, 34–46 (2007)
13. Li, C., Yap, C., Pion, S., Du, Z., Sharma, V.: The Core Library. http://cs.nyu.edu/exact/core_pages/downloads.html
14. Mehlhorn, K., Näher, S.: The LEDA Platform for Combinatorial and Geometric Computing. Cambridge University Press (1999)
15. Schinzel, A., Sierpinski, W.: Elementary Theory of Numbers (Second Edition). North-Holland Mathematical Library vol. 31 (1988)
16. Yap, C.K., Dube, T.: The Exact Computation Paradigm. In: D.-Z. Du and F. K.Hwang (eds.) Computing in Euclidean Geometry, pp. 452–492. World Scientific Press, Singapore (1995)